

# Synthesis of Tetraoctylammonium-Protected Gold Nanoparticles with Improved Stability

Steven R. Isaacs,<sup>†</sup> Erin C. Cutler,<sup>†</sup> Joon-Seo Park,<sup>‡</sup> T. Randall Lee,<sup>‡</sup> and Young-Seok Shon<sup>\*,†</sup>

Department of Chemistry, Western Kentucky University, Bowling Green, Kentucky 42101, and Department of Chemistry, University of Houston, Houston, Texas 77204

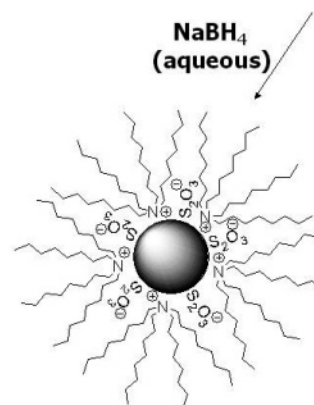
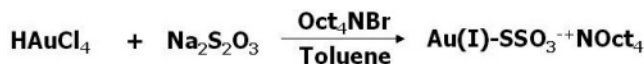
Received March 10, 2005

This paper shows that an introduction of thiosulfate anions in place of bromide anions greatly improves both chemical and thermal stability of tetraoctylammonium-protected gold nanoparticles. Tetraoctylammonium thiosulfate [(Oct)<sub>4</sub>N<sup>+</sup>O<sub>3</sub>SS]<sup>-</sup>-protected gold nanoparticles are synthesized by the reduction of (Oct)<sub>4</sub>N<sup>+</sup>AuCl<sub>4</sub> to Au(I)-SSO<sub>3</sub><sup>-</sup>, followed by the addition of sodium borohydride. The presence of thiosulfate anions instead of bromide anions on the surface of gold nanoparticles results in a significant dampening of the surface plasmon band of gold at 526 nm due to the strong interaction between thiosulfate and the gold nanoparticle surface. Cyanide decomposition and heating treatment studies suggest that (Oct)<sub>4</sub>N<sup>+</sup>O<sub>3</sub>-SS-protected nanoparticles have much higher overall stability compared to (Oct)<sub>4</sub>N<sup>+</sup>Br-protected gold nanoparticles.

## Introduction

Nanoparticles have drawn remarkable interest in the past few years due to their optical and well-defined size-related electronic (e.g., quantized charging) properties.<sup>1,2</sup> Biological applications of hybrid nanoparticles have also shown a great promise for the use of these nanomaterials in biotechnology.<sup>1</sup> Since the first example of the ligand-stabilized gold nanoparticles, Au<sub>55</sub>(PPh<sub>3</sub>)<sub>12</sub>Cl<sub>6</sub>, subsequent investigations were extended to other organic compounds with various reactive headgroups, such as thiol, disulfide, sulfide, thiosulfate, xanthate, phosphine, phosphine oxide, ammonium, amine, carboxylate, selenide, and isocyanide.<sup>1</sup> Thiols have been the most popular choice of protecting monolayers, because thiol-protected nanoparticles exhibit good enough stability to be isolated, redissolved, and handled as molecular reagents.<sup>1,2</sup> However, thiols are believed to poison useful catalytic or biological properties of metal nanoparticles due to their strong interaction with the nanoparticle surface and tendency to form a monolayer with high packing density.<sup>3,4</sup> Tetraalkylammonium bromide-protected metal nanoparticles have drawn an interest for applications which require their labile (or temporary) monolayer binding properties.<sup>5,6</sup> The drawback of tetraalkylammonium protection of nanoparticles has been their unsatisfactory long-term stability.<sup>7</sup> The aggregation or decomposition of monolayer-protected nanoparticles results in the loss of their original properties and prevents the utilization of these nanoparticles for technological applications. Here, we report a facile synthesis of tetra-

## Scheme 1. Synthesis of (Oct)<sub>4</sub>N<sup>+</sup>O<sub>3</sub>SS-Protected Gold Nanoparticles



octylammonium-protected gold nanoparticles with improved chemical and thermal stabilities by introducing thiosulfate (S<sub>2</sub>O<sub>3</sub><sup>2-</sup>) counteranions in place of bromide (Br<sup>-</sup>) anions.

## Experimental Section

**Materials.** The following materials were purchased from the indicated suppliers and used as received: Hydrogen tetrachloroaurate (HAuCl<sub>4</sub>·3H<sub>2</sub>O), sodium borohydride (NaBH<sub>4</sub>), and acetonitrile were purchased from Acros. Tetraoctylammonium bromide and toluene were obtained from Aldrich and Fisher, respectively. Water was purified by a Millipore Simplicity Nanopure Ultrapure water system.

**Synthesis of Tetraoctylammonium-Protected Au Nanoparticles.** Tetraoctylammonium thiosulfate [(Oct)<sub>4</sub>N<sup>+</sup>O<sub>3</sub>SS]<sup>-</sup>-protected gold nanoparticles can be synthesized using a modified Schiffrin reaction (Scheme 1).<sup>8</sup> Briefly, 0.39 g (1.0 mmol) of HAuCl<sub>4</sub> is dissolved in 40 mL of Nanopure H<sub>2</sub>O, and 1.09 g (2.0 mmol) of (Oct)<sub>4</sub>NBr in 160 mL of toluene is added to the reaction flask. The reaction mixture is stirred for 10 min before the addition of 0.47 g (3.0 mmol) of Na<sub>2</sub>S<sub>2</sub>O<sub>3</sub>. In less than 10 min,

\* To whom correspondence should be addressed. E-mail: young.shon@wku.edu.

<sup>†</sup> Western Kentucky University.

<sup>‡</sup> University of Houston.

(1) Daniel, M.-C.; Astruc, D. *Chem. Rev.* **2004**, *104*, 293–346.

(2) Templeton, A. C.; Wuelfing, W. P.; Murray, R. W. *Acc. Chem. Res.* **2000**, *33*, 27.

(3) Alvarez, J.; Liu, J.; Roman, E.; Kaifer, A. E. *Chem. Commun.* **2000**, 1151–1152.

(4) Eklund, S. E.; Cliffl, D. E. *Langmuir* **2004**, *20*, 6012–6018.

(5) Thomas, K. G.; Kamat, P. V. *J. Am. Chem. Soc.* **2000**, *122*, 2655–2656.

(6) Thomas, K. G.; Zajicek, J.; Kamat, P. V. *Langmuir* **2002**, *18*, 3722–3727.

(7) Tetraoctylammonium bromide-protected nanoparticles tend to aggregate over a period of time (usually less than 2 weeks) when they are dissolved in organic solvents.

(8) Fink, J.; Kiely, C.; Bethell, D.; Schiffrin, D. J. *Chem. Mater.* **1998**, *10*, 922–926.

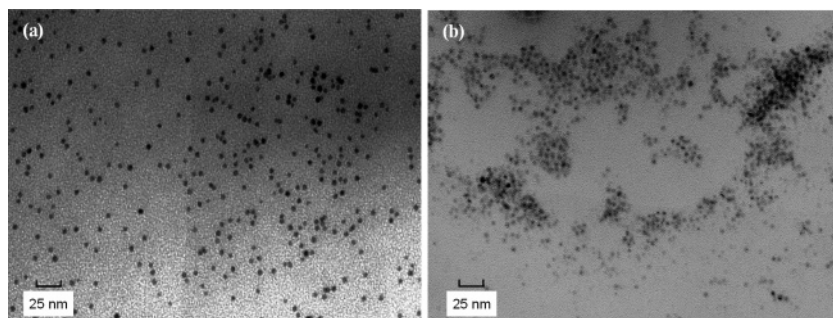


**Figure 1.** TEM images of (a)  $(\text{Oct})_4\text{N}^+-\text{O}_3\text{SS}$ - and (b)  $(\text{Oct})_4\text{N}^+-\text{Br}$ -protected gold nanoparticles ( $\sim 62.5$  mM based on Au for both nanoparticles).

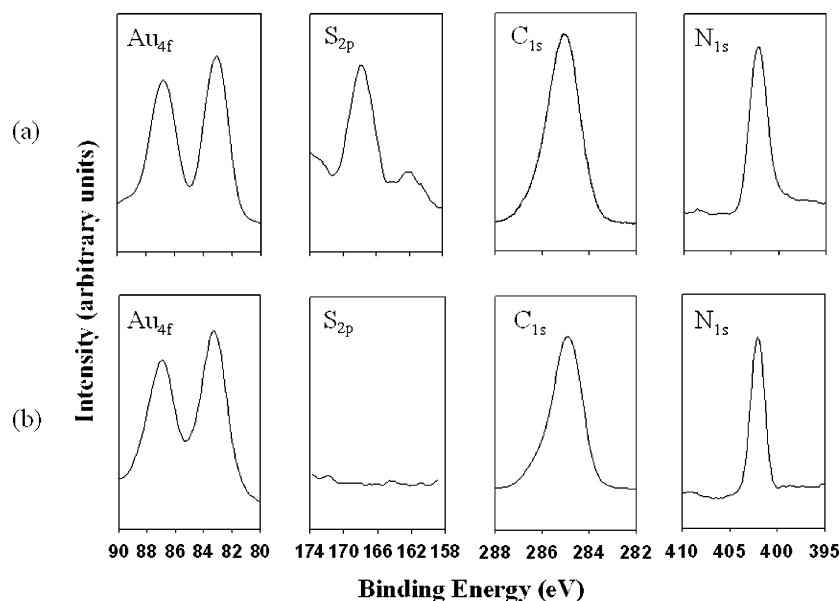


**Figure 2.** XPS Spectra of (a)  $(\text{Oct})_4\text{N}^+-\text{O}_3\text{SS}$ -protected gold nanoparticles and (b)  $(\text{Oct})_4\text{N}^+-\text{Br}$ -protected gold nanoparticles.

a loss of solution color, from red-orange to clear, is observed. This indicates the reduction of Au(III) to Au(I) by  $\text{S}_2\text{O}_3^{2-}$  and results in the formation of thiosulfato-gold(I), which has been used clinically for the treatment of rheumatoid arthritis.<sup>9</sup> After the removal of the aqueous layer, the addition of 0.38 g (10 mmol) of  $\text{NaBH}_4$  causes a fast darkening of solution (brown/purple solution), indicating the nanoparticle formation.  $^1\text{H}$  NMR (270 MHz,  $\text{CDCl}_3$ ):  $\delta$  3.34 (2H, broad,  $\text{NCH}_2$ ), 1.66 (2H, broad,  $\text{NCH}_2\text{CH}_2$ ), 1.45–1.20 (m, 10H), 0.86 (3H,  $\text{CH}_3$ ). IR: 2921  $\text{cm}^{-1}$  ( $\nu_{\text{a}}\text{CH}_2$ ), 2851  $\text{cm}^{-1}$  ( $\nu_{\text{s}}\text{CH}_2$ ), 1457  $\text{cm}^{-1}$  ( $\text{CH}_2$  bending).

Tetraoctylammonium bromide [ $(\text{Oct})_4\text{N}^+-\text{Br}$ ]-protected gold nanoparticles are synthesized by the same procedure without the addition of  $\text{Na}_2\text{S}_2\text{O}_3$ .<sup>8</sup> The reduction of  $(\text{Oct})_4\text{N}^+-\text{AuCl}_4$  complexes with  $\text{NaBH}_4$  results in the formation of nanoparticles. The resulting solution containing  $(\text{Oct})_4\text{N}^+-\text{Br}$ -protected gold nanoparticles exhibits a strong purple/red color.

**Measurements.** Proton NMR spectra were recorded on a JEOL CPX FT-NMR spectrometer operating at 270 MHz in  $\text{CDCl}_3$  solutions and internally referenced to  $\delta$  7.26. Infrared spectra were obtained, using a Perkin-Elmer 1600 FT-IR spectrometer, of films of MPCs pressed into a KBr plate. The spectra were recorded from 4500 to 450  $\text{cm}^{-1}$ . X-ray photoelectron spectroscopy (XPS) spectra were collected using a PHI 5700 X-ray photoelectron spectrometer equipped with a monochromatic Al  $K\alpha$  X-ray source ( $h\nu = 1486.7$  eV) incident at  $90^\circ$  relative to the axis of a hemispherical energy analyzer.<sup>10</sup> The binding energies were referenced by setting the C(1s) binding energy to 285.0 eV. UV-vis spectra of toluene solutions in quartz cells were acquired on a Shimadzu UV-2101 PC spectrophotometer. Transmission electron microscopy (TEM) images of nanoparticles were obtained

with a JEOL 120CX scanning/transmission electron microscope operating at 120 keV. Samples were prepared for TEM by casting a single drop of a  $\sim 1$  mg/mL toluene solution onto standard carbon-coated (80–100 Å) Formvar film on copper grids (600 mesh) and drying in air for at least 30 min. Several regions were imaged at 100 000 $\times$ . Size distributions of the gold cores were obtained from digitized photographic enlargements with Scion Image Beta Release 2.

**Cyanide Decomposition of Nanoparticles.** A 3 mL sample of tetrahydrofuran solutions of  $(\text{Oct})_4\text{N}^+-\text{O}_3\text{SS}$ -protected gold nanoparticles (final concentration ca. 7.1 mM in particle) is quickly mixed with 0.5 mL of an aqueous NaCN solution (final concentration of ca. 2.2 mM). The decay in absorbance (at  $\gamma = 525$  nm) is monitored over at least three reaction half-lives on a Shimadzu UV-2101 PC spectrophotometer, as the light brown particle solution decomposes into one containing colorless, slightly soluble cyano-Au complexes (assumed, actual identity of Au product not determined) and tetraoctylammonium complexes. The kinetics of cyanide decomposition of  $(\text{Oct})_4\text{N}^+-\text{Br}$ -protected gold nanoparticles is studied simultaneously.

**Heating Treatments of Nanoparticles.** The heating treatment was performed with toluene solutions containing  $(\text{Oct})_4\text{N}^+-\text{O}_3\text{SS}$ - or  $(\text{Oct})_4\text{N}^+-\text{Br}$ -protected gold nanoparticles (ca. 0.006 25 M Au) in a temperature range from room temperature up to the boiling point of toluene (111  $^\circ\text{C}$ ). The solution was heated in a silicone oil bath with controlled temperature. The bath was maintained at a constant temperature during the entire heating process.

## Results and Discussion

**TEM.** TEM results of these two nanoparticles (Figure 1) show that both particles are spherical in shape and have similar average core size [ $4.8 \pm 0.9$  nm for

(9) Shaw, C. F., III. *Chem. Rev.* **1999**, *99*, 2589–2600.

(10) Park, J.-S.; Smith, A. C.; Lee, T. R. *Langmuir* **2004**, *20*, 5829–5836.

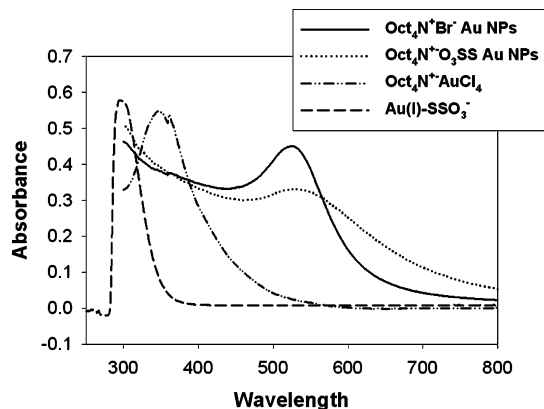


**Figure 3.** UV-vis Spectra of  $(\text{Oct})_4\text{N}^+\text{-AuCl}_4$ ,  $\text{Au(I)-SSO}_3^-$ , and  $(\text{Oct})_4\text{N}^+\text{-O}_3\text{SS-}$  and  $(\text{Oct})_4\text{N}^+\text{-Br-}$  protected gold nanoparticles in toluene ( $\sim 1$  mM based on Au).

$(\text{Oct})_4\text{N}^+\text{-O}_3\text{SS-}$  and  $5.0 \pm 1.0$  nm for  $(\text{Oct})_4\text{N}^+\text{-Br-}$  protected gold nanoparticles]. Some spacing between close particles indicates the presence of organic monolayers.  $(\text{Oct})_4\text{N}^+\text{-O}_3\text{SS-}$  protected gold nanoparticles are very discrete and not fused into larger aggregates, showing that these nanoparticles have comparable stability with alkanethiol-protected gold nanoparticles at room temperature. In comparison, the TEM image of  $(\text{Oct})_4\text{N}^+\text{-Br-}$  protected gold nanoparticles exhibits the presence of some fused particle domains upon solvent evaporation.

**XPS.** The analysis of monolayer-protected nanoparticles by XPS can provide information regarding both the chemical composition of the nanoparticles and the nature of the chemical bond between the adsorbate headgroups and the surface.<sup>11</sup> Examination of S(2p) binding energies is of particular importance for our study (Figure 2). Analysis of the  $(\text{Oct})_4\text{N}^+\text{-O}_3\text{SS-}$  protected gold nanoparticles clearly shows the presence of sulfur bound to the gold surface at  $\sim 162$  eV [S(2p<sub>3/2</sub>)] and oxidized sulfur species at  $\sim 167$  eV [S(2p<sub>1/2</sub>)]. In comparison, XPS spectra of  $(\text{Oct})_4\text{N}^+\text{-Br-}$  protected gold nanoparticles confirms the absence of any sulfur species on these nanoparticles. Other binding energies such as Au(4f) ( $\sim 84$  eV), C(1s) ( $\sim 285$  eV), and N(1s) ( $\sim 402$  eV) are almost identical for both ionic gold nanoparticles (Figure 2).

**UV-Vis Spectroscopy.**  $(\text{Oct})_4\text{N}^+\text{-AuCl}_4$  complexes have a strong absorption band at 347 nm as shown in UV-vis spectra (Figure 3). This absorption band is characteristic of the metal-to-ligand charge-transfer band of  $\text{AuCl}_4^-$ .<sup>6</sup> Addition of  $\text{Na}_2\text{S}_2\text{O}_3$  causes a blue shift in absorbance and results in the appearance of a strong absorption band of  $\text{Au(I)-SSO}_3^-$  at 302 nm. The reduction of  $(\text{Oct})_4\text{N}^+\text{-AuCl}_4$  complexes with  $\text{NaBH}_4$  yields  $(\text{Oct})_4\text{N}^+\text{-Br-}$  protected gold nanoparticles. On the other hand, the reduction of  $\text{Au(I)-SSO}_3^-$  results in the formation of  $(\text{Oct})_4\text{N}^+\text{-O}_3\text{SS-}$  protected gold nanoparticles. UV-vis data of  $(\text{Oct})_4\text{N}^+\text{-Br-}$  protected gold nanoparticles show a strong surface plasmon (SP) band of gold at 526 nm. In contrast, UV-vis data of  $(\text{Oct})_4\text{N}^+\text{-O}_3\text{SS-}$  protected gold nanoparticles exhibit a significant dampening of the gold SP band, but it is still visible at 526 nm. Because the average core dimensions of these two nanoparticles are almost identical, which is evidenced by TEM results, the discrepancy in the intensity of two gold SP bands should be resulted from the difference in interaction of monolayers with the gold nanoparticle surface.<sup>6</sup> Binding of gold nanoparticles with organic molecules containing functional groups such as  $-\text{SCN}$  or

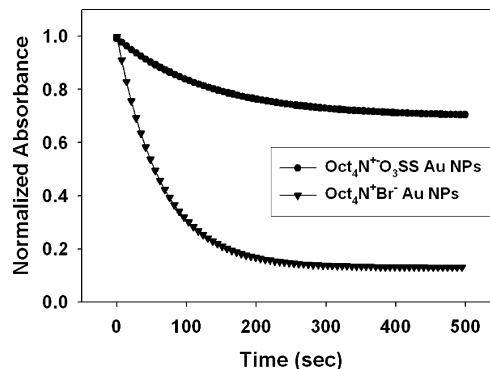


**Figure 4.** Kinetics studies on the cyanide decomposition of  $(\text{Oct})_4\text{N}^+\text{-O}_3\text{SS-}$  and  $(\text{Oct})_4\text{N}^+\text{-Br-}$  protected gold nanoparticles using UV-vis spectroscopy.

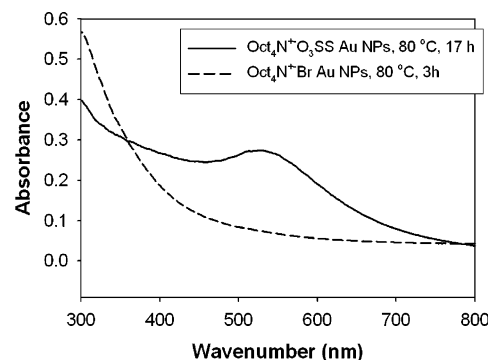


**Figure 5.** UV-vis spectra of  $(\text{Oct})_4\text{N}^+\text{-O}_3\text{SS-}$  and  $(\text{Oct})_4\text{N}^+\text{-Br-}$  protected gold nanoparticles after heating treatment at  $80^\circ\text{C}$ .

$-\text{NH}_2$  was found to dampen the SP bands.<sup>6</sup> This UV-vis data suggest that there is a strong interaction between the gold nanoparticle surface and anions for  $(\text{Oct})_4\text{N}^+\text{-O}_3\text{SS-}$  protected gold nanoparticles.

**Cyanide Decomposition.** Chemical stability of monolayer-protected metal nanoparticles can be measured by using a cyanide decomposition reaction, which the rate of core decay indicates a measure of core protection.<sup>12,13</sup> It has been found that the reaction is first-order in both the concentration of the clusters and the concentration of cyanide in solutions. The absorbance decay data are fitted to a general first-order equation,  $y = y_0 + ae^{-kt}$ , where  $y$  is the experimental absorbance and  $y_0$  is a constant term accounting for a small amount of absorbance and/or light scattering by the reaction product. Figure 4 shows the decay of solution absorbance at 525 nm. The rate constant ( $2.9 \times 10^{-1} \text{ M}^{-1} \text{ s}^{-1}$ ) of  $(\text{Oct})_4\text{N}^+\text{-O}_3\text{SS-}$  protected gold nanoparticles was found to be less than those ( $8.7 \times 10^{-1} \text{ M}^{-1} \text{ s}^{-1}$ ) obtained from  $(\text{Oct})_4\text{N}^+\text{-Br-}$  protected gold nanoparticles. This result clearly indicates that the presence of thiosulfate ( $\text{S}_2\text{O}_3^{2-}$ ) anions in place of bromide anions provides a better protection against chemical etching due to the stronger interaction of thiosulfate anions with the gold nanoparticle surface.

**Heating Treatments.** Thermal stability of  $(\text{Oct})_4\text{N}^+$  protected gold nanoparticles is also being studied by performing thermal treatments of dilute (6.25 mM based on Au) particle solution in toluene. The UV-vis results (Figure 5) show that  $(\text{Oct})_4\text{N}^+\text{-Br-}$  protected gold nanoparticles decompose at  $80^\circ\text{C}$  after thermal treatment of less than 3 h. In contrast, thermal treatment of

(11) Shon, Y.-S.; Gross, S. M.; Dawson, B.; Porter, M.; Murray, R. W. *Langmuir* **2000**, *16*, 6555–6561.

(12) Templeton, A. C.; Hostetler, M. J.; Kraft, C. T.; Murray, R. W. *J. Am. Chem. Soc.* **1998**, *120*, 1906–1911.

(13) Paulini, R.; Frankamp, B. L.; Rotello, V. M. *Langmuir* **2002**, *18*, 2368–2373.

(Oct)<sub>4</sub>N<sup>+</sup>-O<sub>3</sub>SS-protected gold nanoparticles at the same temperature for more than 17 h has no effect on the intensity and wavelength of the gold SP band. Further study shows that (Oct)<sub>4</sub>N<sup>+</sup>-O<sub>3</sub>SS-protected gold nanoparticles do not decompose by the solid-state thermal treatment at 150 °C for up to 3 h. These results suggest that the thermal stability of (Oct)<sub>4</sub>N<sup>+</sup>-O<sub>3</sub>SS-protected gold nanoparticles is quite comparable to that of alkanethiolate-protected gold nanoparticles.<sup>14,15</sup>

### Conclusion

An introduction of thiosulfate anions to tetraoctylammonium-protected gold nanoparticles greatly enhances

---

(14) Shimizu, T.; Teranishi, T.; Hasegawa, S.; Miyake, M. *J. Phys. Chem. B* **2003**, *107*, 2719–2724.

(15) Maye, M. M.; Zheng, W.; Leibowitz, F. L.; Ly, N. K.; Zhong, C.-J. *Langmuir* **2000**, *16*, 490–497.

both the chemical and the thermal stability of nanoparticles. The availability of more stable monolayer-protected nanoparticles with an ionic bonding between protecting ligands and the particle surface might provide a diversification of available nanoparticulate materials and potential applications. The detailed characterization, manipulation, and application of these new nanoparticles are currently being investigated.

**Acknowledgment.** This research was supported by grants from Research Corporation (Cottrell College Science Award) and Western Kentucky University. We thank Dr. John Andersland for assistance with TEM.

LA050656B